Copyright © 2011 by ABCM

PROJECT OPTIMIZATION OF HIGH-PERFORMANCE AXIAL FLOW COMPRESSOR USING MULTI-OBJECTIVE GENETIC ALGORITHM SEARCH

Victor Fujii Ando, victor.ando@gmail.com
João Roberto Barbosa, barbosa@ita.br
Instituto Tecnológico de Aeronáutica. DCTA-ITA-IEM Grupo de Turbinas, São José dos Campos-SP, CEP 12228-900

Nelson Manzanares Filho, nelson@unifei.edu.br
Universidade Federal de Itajubá

Abstract. *This work presents a proposal for project optimization of high-performance axial flow compressor. Through integration of a specially developed computational program based on the streamline curvature method and an optimization software, many compressor designs were performed using the Multi-Objective Genetic Algorithm. A search proceeded for compressors with high efficiencies and low diffusion factor, as well as, low camber angle. To obtain new designs, the stator outlet blade angles were varied using a bilinear multivariate interpolation simplification. Additionally, the hub to tip ratio was also varied. Eventually, the search revealed two notable designs, which not only are from the Pareto front, but also their diffusion and camber angle characteristics are within a chosen restricted acceptable range. Afterwards, a comparison between the compressors obtained via Genetic Algorithm search and the initial non-optimized compressor reveals an improved design. However considerable modifications might be required due to high outlet gas angle prior to the combustion chamber.*

Keywords*: Axial flow compressor, optimization, genetic algorithm*

1. INTRODUCTION

The research on gas turbines at Instituto Tecnológico de Aeronáutica (ITA) takes place within the Centre for Reference on Gas Turbine and Energy (CRTGE – Centro de Referência em Turbinas a Gás e Energia). The development of technologies related to gas turbines is lengthy and costly, thus the industries and research institutes treat the results and correlations derived from experiments as confidential, as they represent key elements on their competitiveness. The research conducted within CRTGE is based upon information of public domain, although still relatively restricted, and upon many years of experience of its members. The centerpiece of the research developed in CRTGE is on numerical simulation of performance.

The study on compressor design optimization of compressor intends to provide a better understanding of the impact of many geometrical parameters on the achievement of high efficiencies, more appropriate dimensions and even reduced costs. Even though the theme of research on optimization in engineering is not internationally new, it is relatively recent among the groups that work with gas turbines and aim at the development of design technology and design of those machines.

Compressor design is a difficult task that involves past experience. Usually, the designer takes the design parameters from tests that lead to good performance, however may not deliver the best. Compressor geometry optimization has been the object of more recent research (Oyama, 2002; Ando, 2010). Among the design process, the one that is based on the Streamline Curvature is well accepted, due to its intrinsic characteristics of simplicity, convergence and robustness. The code developed at ITA revealed to be appropriate for the optimization process.

2. OBJECTIVE

The objective of this work is to present a procedure to optimize the project of a high-performance axial flow compressor. To achieve it, certain geometric parameters were chosen and varied aiming at efficiency increase. An in-house developed program for design, based on the streamline curvature method, developed by Barbosa (1987), is fully operational. The search for more efficient compressors was achieved by the integration of this program to the Multi-Objective Genetic Algorithm (MOGA-II).

3. NOMENCLATURE

There exist many distinct notations concerning geometry and aerodynamic aspects of gas turbines. Thus, it is relevant to start with the clarification of the symbols used henceforth. The nomenclature used in this work is the same as from Saravanamutto (1996) and is indicated in Fig. 1.

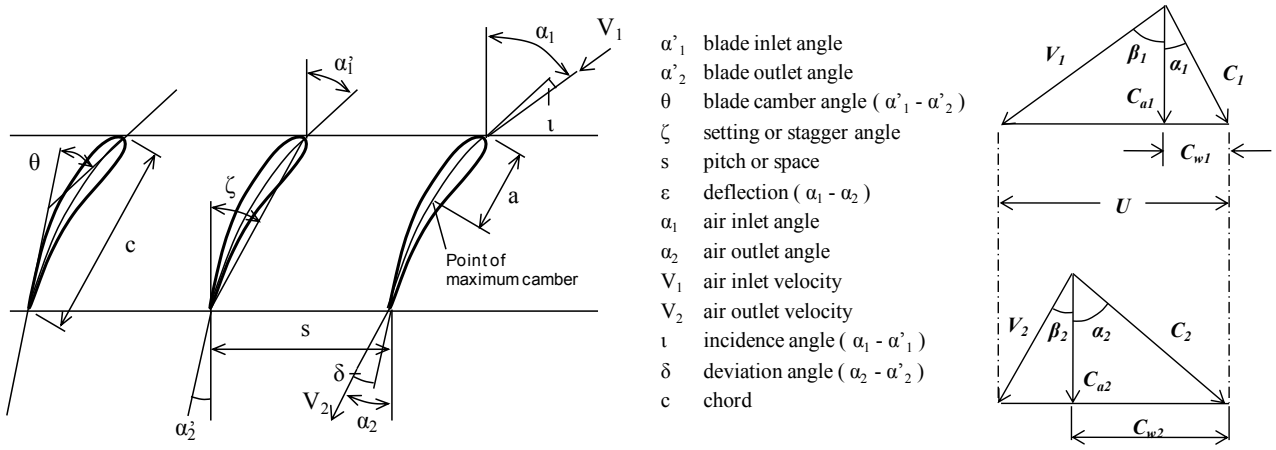

Figure 1. Nomenclature used in this work.

4. THE STREAMLINE CURVATURE METHOD

This work intends to provide a simplified method to optimize the performance of an axial-flow compressor. For that, an optimization routine is coupled to the performance computational program named Streamline Curvature Computational Programme (SCCP). This section is intended to briefly explain the computational program developed by Barbosa (1987) and revised and further developed by Figueiredo (2010), which was used in the performance calculations node of the optimization project. Since the program contains many parts, the discussion here will not go into details.

The streamline curvature method basically consists of writing the flow equations in a streamline-blade edge coordinate system (m-s). Those coordinates are schematically shown in Fig. 2.

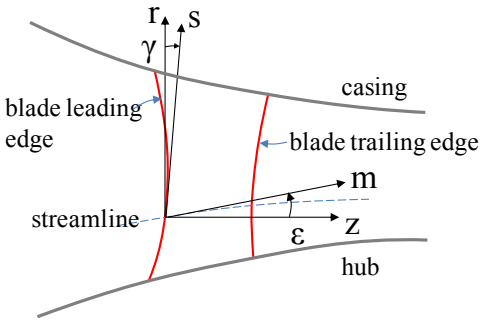

Figure 2. Streamline-blade edge (m-s) coordinate system.

The non-viscous momentum equation in a non-inertial referential frame can be written as follows:

$$-\frac{1}{\rho}\nabla P = \frac{D\mathbf{V}}{Dt} + \boldsymbol{\omega}\times\boldsymbol{\omega}\times\mathbf{r} + 2\boldsymbol{\omega}\times\mathbf{V} + \mathbf{F} \tag{1}$$

where P is the static pressure, $\mathbf{V}$ is the velocity field, $\boldsymbol{\omega}$ is the angular velocity and $\mathbf{F}$ is an external force. The material derivative is given by

$$\frac{D\mathbf{V}}{Dt} = C_r\frac{\partial\mathbf{V}}{\partial r} + \frac{V_\theta}{r}\frac{\partial\mathbf{V}}{\partial\theta} + V_z\frac{\partial\mathbf{V}}{\partial z}. \tag{2}$$

Combining Eq. (1) and Eq. (2), and writing each coordinate (in cylindrical coordinates) separately, one has:

$$-\frac{1}{\rho}\frac{\partial P}{\partial r} = C_r\frac{\partial C_r}{\partial r} + \frac{V_\theta}{r}\frac{\partial C_r}{\partial\theta} + V_z\frac{\partial C_r}{\partial z} - \frac{V_\theta^2}{r} - \omega^2 r - 2\omega V_\theta, \tag{3}$$

$$-\frac{1}{r\rho}\frac{\partial P}{\partial \theta}=C_r\frac{\partial V_\theta}{\partial r}+\frac{V_\theta}{r}\frac{\partial V_\theta}{\partial \theta}+C_z\frac{\partial V_\theta}{\partial z}+\frac{C_rV_\theta}{r}+2\omega C_r, \tag{4}$$

$$-\frac{1}{\rho}\frac{\partial P}{\partial z}=C_r\frac{\partial C_z}{\partial r}+\frac{V_\theta}{r}\frac{\partial C_z}{\partial \theta}+C_z\frac{\partial C_z}{\partial z}, \tag{5}$$

Barbosa (1987) develops Eqs. (3) to (5) in the aforementioned s-m coordinates. Eventually, Eqs. (6) and (7) are obtained.

$$C_m\frac{\partial C_m}{\partial s}=\cos^2(\beta)\left\{\left[\frac{\partial I}{\partial s}-T\frac{\partial S}{\partial s}\right]+V_m^2\left[\begin{array}{l}\dfrac{\cos(\varepsilon+\gamma)}{R_c}-\dfrac{\tan(\beta)}{\cos^2(\beta)}\dfrac{\partial \beta}{\partial s}+\dfrac{2U}{V_m}\tan(\beta)\dfrac{\cos(\beta)}{r}- \\ -\tan^2(\beta)\dfrac{\cos(\gamma)}{r}+\dfrac{\sin(\varepsilon+\gamma)}{V_m}\dfrac{\partial V_m}{\partial m}\end{array}\right]\right\}, \tag{6}$$

where

$$C_m\frac{\partial C_m}{\partial m}=\frac{C_m^2}{\left(1-M_m^2\right)}\left\{-\sec(\varepsilon+\gamma)\frac{\partial \varepsilon}{\partial s}+\frac{\tan(\varepsilon+\gamma)}{R_c}+\frac{1}{R}\frac{\partial S}{\partial m}-\left(1+M_m^2\right)\frac{1}{r}\sin(\varepsilon)\right\} \tag{7}$$

Equations (6) and (7) form a system of partial differential equations and are integrated along the streamlines. The system can be solved if it is previously know that flow properties vary smoothly at the blade edges.

Additionally, many correlations derived from experimental research were incorporated in order to correct the model, which is initially inviscid. The losses are incorporated when the calculation proceeds from the leading edge to the trailing edge making corrections to the total pressure. Details of the loss model can be found in Barbosa (1987).

A flow blockage correlation is used to add the effect of the compressor annulus area decrease due to the boundary layer formation. Mass continuity equation in both differential and integral form is integrated to evaluate the flow acceleration and the mass flow inside the streamtubes. A choking expression is implemented to stop the calculations in case of choking, which can occur either in the annulus or in the passage throat. Finally, stall and surge correlations are integrated, as well.

The program incorporates three commonly used types of blade sections, namely, double circular arc (DCA), NACA 65 series (65S) and British C series (C4). User-defined blade sections are also a possibility in the program.

The incidence at which minimum loss occurs is calculated both via NASA minimum loss incidence model and via the unique incidence, for modern compressors, which run sonic and supersonic flows, accordingly. A similar approach of calculation of deviation for modern compressors is conducted, as well.

4.1. Loss model

The loss model adopted in the design program of Barbosa (1987) assumes that the total pressure loss is due to profile, secondary and shock losses. A successful performance prediction relies on the loss model and on the deviation rule, as the flow is highly dependent upon them. It was chosen to associate the diffusion factor with losses due to a more realistic representation of the loss variation near the walls.

4.1.1. Profile loss

The computational program gives the user the option of two diffusion models: Swan (1961) and Monsarrat et al. (1969). Both authors produced a set of curves of losses and diffusion factor, but the former offers a more actual distribution.

Monsarrat's model, which is defined only for the design condition, takes account of radial variation of the diffusion factor.

$$D^*=1-\frac{C_2^*}{C_1^*}+\frac{r_1}{r_1+r_2}\frac{s}{c}\left[\tan\left(\beta_1^*\right)-\frac{r_2}{r_1}\frac{C_{m2}^*}{C_{m1}^*}\tan\left(\beta_2^*\right)\right] \tag{8}$$

and computing the minimum loss parameter $\overline{\omega}_p^*$

$$\left(\frac{\theta}{c}\right)^* = \overline{\omega}_p^* \frac{s}{c} \frac{\cos(\beta_2)}{2} \tag{9}$$

where θ is the trailing edge boundary layer momentum thickness, obtained from a correlation that can be found in the work of Monsarrat.

If the diffusion factor increases, there is a tendency of stalling and of growth of the boundary layer, thus, decrease in the capability of stage pressure rise. As a result, the losses increase with the increase of the diffusion factor. Therefore, in the optimization process, the diffusion factor is a parameter to be controlled. Usual practice suggests that this value should not exceed 0.600, then a penalty factor will be defined for designs which exceed this values. This procedure will be further detailed in section 7.2.

4.1.2. Secondary loss

Secondary loss is caused by secondary flows inside the blade passages. The model used in this work is the one developed by Griepentrog (1970). An approximation is made to the flow in cascade blade passages and the induced drag due to trailing edge vortices, taking account of space-chord ratio, boundary layer thickness and shape factor.

4.1.3. Shock loss

Shock loss is caused by shock waves at the channel inlet. The NASA SP-36 model is used in this work. An approximation is made to the flow in the blade passages assuming average Mach number resulted from the inlet flow and the accelerated flow over the suction surface of the blade, caused by Prandtl-Meyer expansion.

4.2. Hub to tip ratio

The hub to tip ratio ($htr=r_h/r_t$, radius at the hub divided by the radius at the tip), is related to the compressor frontal area and the length. The greater the htr, the greater the frontal area, for a fixed intake area. There is, however, a lower limit of between 30% or 35%, below which an adequate fixation of the blades on the hub is compromised.

There is also an upper limit, since high values for *htr* results in tiny blades. Consequently, the losses due to tip clearance increase significantly. A high value of *htr* results in an inconvenient geometry of the rotor concerning the bend of the flow entering the compressor at the height of the blade root. This inconvenience leads to the requirement of a long bullet.

The choice of the *htr* depends also on the mean diameter of the combustion chamber inlet. Another overall geometrical consequence is the compressor length: the higher the *htr*, the shorter the compressor if the *h/c* is fixed.

5. MULTI-OBJECTIVE GENETIC ALGORITHM (MOGA) OPTIMIZATION

Genetic algorithms (GAs) are search and optimization procedures based on the mechanics of natural selection and natural genetics. The fundamental principles of genetics are adapted to create a population, which reproduces, mutates, suffers crossing over and are then selected according to a survival criterion. Briefly, a simple GA is composed by three operators, namely: Reproduction, Crossover and Mutation. The basic structure of a GA algorithm is given by Deb (2002) in Fig. 3.

In single-objective problems, the fitness of an individual is given by its objective function value. To treat multi-objective problems, a new approach is required. Instead of analyzing each objective, and perhaps attributing multiple fitness values, the fitness is related to the rank of each solution. The rank of a certain solution is simply one plus the number of solutions that dominates this solution.

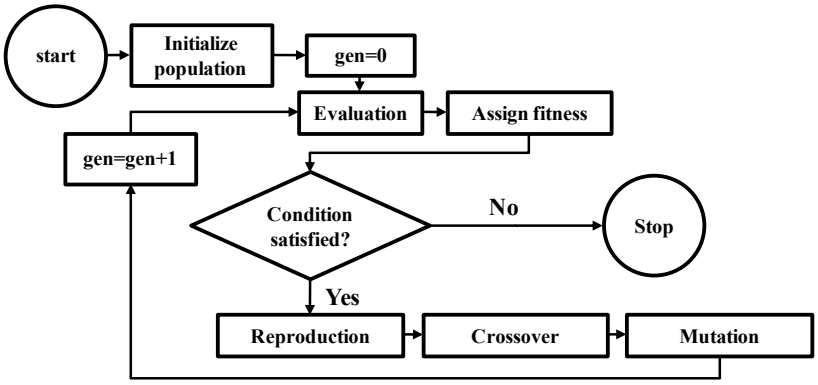

Figure 3. Working principle of a Genetic Algorithm, according with Deb (2002).

MOGA does also have corrections in the fitness to secure diversity among non-dominated solutions. In order to detail this procedure, the sharing function is defined as follows:

$$Sh(d) = \begin{cases} 1 - \left(\dfrac{d}{\sigma_{share}} \right)^{\alpha}, & \text{if d} \le \sigma_{share}; \\ 0, & \text{otherwise.} \end{cases}, \tag{10}$$

where d is the distance between any two solutions in the population and σ_{share} is a distance, which determines a region wherein the sharing function assumes a value greater than zero. One can note that the sharing functions assumes values in the interval [0,1]. Next, a function called niche count is calculated. This function is the sum of all the sharing functions of solution i, including i itself:

$$nc_i = \sum_{j=1}^{N} Sh(d_{ij}). \tag{11}$$

For a Multi-Objective Optimization Problem (MOOP), the distance between any two solutions i and j in a rank is calculated as:

$$d_{ij} = \sqrt{\sum_{k=1}^{M} \left(\frac{f_k^{(i)} - f_k^{(j)}}{f_k^{\max} - f_k^{\min}} \right)}, \tag{12}$$

where $f_k^{\max}$ and $f_k^{\min}$ are the maximum and minimum objective functions values of the k-th objective. For the solution i, the distance is calculated for every solution j, which includes i, with the same rank. Additionally, the summation upper limit N in Eq. (11) is the number of solutions in rank i, $\mu(r_i)$.

6. METHODOLOGY

To integrate the SCCP to an optimization software, some modifications and strategies were required. Firstly, the SCCP was altered to display nothing during its execution, to exclude user interference during runs. Then, a sub-routine that generates a simplified output file containing only information of interest to the optimization was written. Next, the parameters of interest to the optimization were selected according to the experience of compressor designers. Finally, the optimization workflow was designed, the optimizer was chosen and configured and the initial population was created.

The SCCP receives the isentropic efficiency as input parameter. Then it performs the calculation in order to achieve the given efficiency within a certain margin. In order to maximize the efficiency, it was proposed that the given efficiency should be an input parameter to the optimizer and the calculated efficiency should be the output and objective. As the SCCP controls the difference between given and calculated efficiency with a very tight tolerance, the procedure revealed consistent.

6.1. Geometrical parameters

The chosen geometrical parameters were the hub-to-tip ratio and the stator gas outlet angles at each computational node. As a compressor with five stages and five streamlines was simulated, a total of 50 nodes result. Instead of allowing a variation of all 25 outlet angles, what would require long computational run, a simplification was derived. Only four angles were set as variable parameters: at the root and at the tip of the first stage and at the root and at the tip of the last stage. Then a multivariate bilinear interpolation was carried. Say that the angle at any node is given by *f(i,j)*, where *i* is the stage and *j*, the streamline, $i \in [i_{\min}, i_{\max}]$ and $j \in [j_{\min}, j_{\max}]$, then

$$\begin{aligned} &f(i,j) = a.i.j + b.i + c.j + d \\ &f(i_{\min}, j_{\min}) = f_{ll};\ f(i_{\min}, j_{\max}) = f_{lh}; \\ &f(i_{\max}, j_{\min}) = f_{hl};\ f(i_{\max}, j_{\max}) = f_{hh}. \end{aligned} \tag{13}$$

Solving (14), it follows:

$$\begin{aligned} f(i,j) = &\left[\frac{f_{hh} - f_{hl} - f_{lh} + f_{ll}}{(i_{\max} - i_{\min})(j_{\max} - j_{\min})}\right] ij + \left[\frac{f_{hl} j_{\max} - f_{ll} j_{\max} + (-f_{hh} + f_{lh}) j_{\min}}{(i_{\max} - i_{\min})(j_{\max} - j_{\min})}\right] i + \\ &+ \left[\frac{f_{lh} i_{\max} - f_{ll} i_{\max} + (-f_{hh} + f_{hl}) i_{\min}}{(i_{\max} - i_{\min})(j_{\max} - j_{\min})}\right] j + \left[\frac{f_{ll} i_{\max} j_{\max} - f_{hl} i_{\min} j_{\max} + (-f_{lh} i_{\max} + f_{hh} i_{\min}) j_{\min}}{(i_{\max} - i_{\min})(j_{\max} - j_{\min})}\right]. \end{aligned} \tag{14}$$

6.2. Camber angle

The blade camber angle, $\theta = \alpha' - \alpha'_2$, is associated with stall, due to the change in the gas direction under deceleration. A high camber angle is desired, but the channel formed by the blades should also not be long, because of the increase in friction losses. In summary, the choice of the camber angle is a compromise between friction losses and chord length. Usual practice suggests a value not greater than 40°. Values which exceed 40° should be avoided, thus a penalty factor similar to the penalty factor to the diffusion factor was defined.

6.3. Penalty factor

Initial optimization procedures were providing compressors with very high efficiencies, and it was an easy task to obtain designs with circa 95% efficiency. Nevertheless, conducting a thorough analysis on fluid properties and geometrical blade parameters showed that those 'efficient' designs were actually unfeasible.

The most critical violations were found to be on the diffusion factor, which should not be greater than 0.600 using Monsarrat Model, and on the camber angle, which should not be greater than 40°. A high value of diffusion factor is related to losses due to high loading of the row. And high values of camber angle imply stall.

To overcome this inconsistency, the program was modified to penalize unfeasible designs. The approach was simply to sum the amount of each of those properties at each node which were greater than a specified value, say 0.600 for the diffusion using Monsarrat and 40° for the camber angle.

Even though those parameters are restrictions, they were treated as objectives to be minimized. This approach was chosen, because previous tests taking them as restrictions (penalizing the solutions) caused problems in generating an initial set of population. The restriction approach was too selective and killed most of the solutions. Differently, the objective approach allowed unfeasible solutions, but the existence of a reasonable number of individuals resulted in a better search for solutions, which eventually were feasible.

6.4. Optimization setup

The initial population set in the Design of Experiments (DOE) is given by the Latin Square. It was chosen six levels, resulting in 36 designs.

The chosen optimizer was the MOGA-II with the settings given by Tab.1.

The input parameters and their intervals, as well as the steps are shown in Tab.2. Notably, a considerable variation was allowed for the angles. Although it is not common optimization practice, this study intends to search different compressor configurations, as well.

Table 1. MOGA-II settings.

Optimizer	MOGA-II
Number of generations	50
Probability of directional cross-over	0.5
Probability of selection	0.05
Probability of mutation	0.1
DNA string mutation ratio	0.05
Elitism	Enabled
Number of concurrent design evaluations	24
Evaluate repeated designs	No

Table 2. Input parameters range and step.

Parameter	Lower bound	Upper bound	Step
Isentropic efficiency	0.800	0.920	0.001
f_{ll}	0.0	60.0	0.1
f_{lh}	0.0	60.0	0.1
f_{hl}	0.0	60.0	0.1
f_{hh}	0.0	60.0	0.1
Hub to tip ratio	0.400	0.600	0.001

7. RESULTS AND ANALYSIS

7.1. Initial non-optimized compressor

The optimization procedure was carried to obtain a better solution than the solution which was previously obtained with demanding efforts of multiple tries and project experience. Relevant parameters that are kept constant in the optimization are listed in Tab. 4. The variable parameters configuration of the initial compressor is found in Tab. 3 and the summarized results are given in Tab. 5.

Table 3. Initial compressor design – input parameters

Parameter	Value
Given isentropic efficiency	0.85
Hub to tip ratio	0.55
Stator outlet angle distribution	Matrix – all angles with 25°

Table 4. Fixed relevant parameters.

Parameter	Value
Ambient pressure	101325 Pa
Pressure ratio	5.000
Number of stages	5
Mass flow	8.20 kg/s
Blade profile	DCA
Tip clearance	1%
Minimum space between rows	0.0100

Table 5. Initial compressor design results.

Parameter	Value
Compressor length	0.2383
Calculated efficiency	0.8508
Diffusion penalty	0.18
Camber angle penalty	84.90

Although a reasonable diffusion penalty of 0.18 was obtained, the camber angle penalty of 84.90 was definitely quite high. In Fig. 4, red indicates the first row; green, the second; blue, the third; light brown, the fourth; and dark

cyan, the fifth. Circle markers indicate rotors and triangular markers indicate stator. The same colour and marker scheme will be used hereafter; hence, the legend will be omitted.

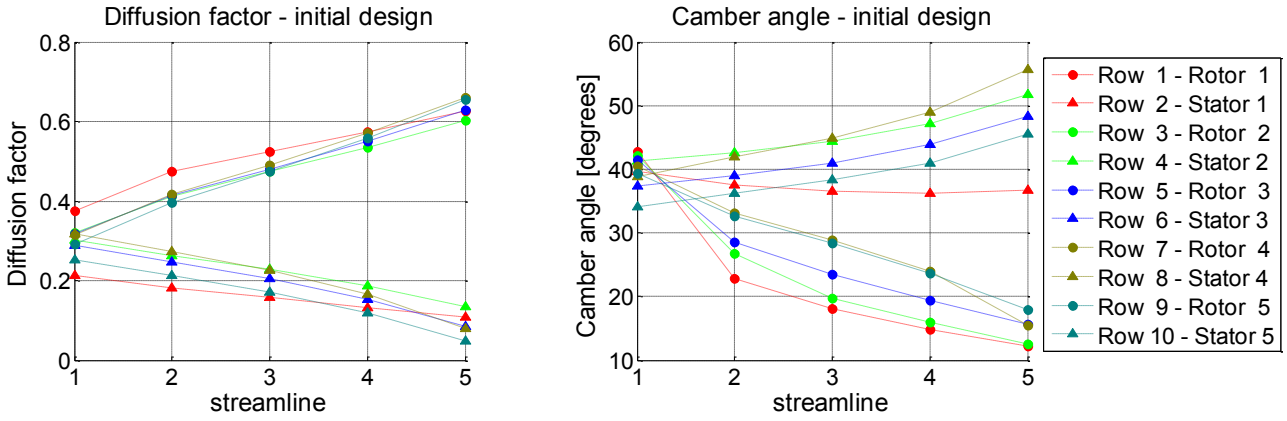

Figure 4. High values of diffusion factor (left) and camber angle (right).

It is interesting to note that the diffusion factor increases from root to tip at the rotors and decrease at the stators. It should be regarded that the outermost streamlines (j=5) at the rotors have a diffusion factor greater than 0.600, what is definitely not desirable.

The camber angle result shows a compressor with serious potential problems of stall. Not only are there as many as 18 nodes with camber angle greater than the determined limit of 40°, which represent 36% of the nodes, but also many of them overly exceed this limit, mainly at the outermost streamlines at the stators.

7.2. More efficient compressors found

The optimization procedure resulted in 1109 feasible designs. Among those, two solutions were of greater interest, because they are from the Pareto front, as well as their camber angle penalty and diffusion factor penalty are both nil. Those solutions are: ID 1594 and ID 1657, whose numbers will easy the reference from here on. They can be seen in the Bubble 4-D diagram of Figure 5, in which the x-axis represents the compressor calculated efficiency; the y-axis represents the compressor length; the bubble diameter represents the camber penalty (*penc*) and the bubble color represents the diffusion penalty according to the color map. Thus, the optimal solution should be found at the bottom of the graph, representing a short compressor; at the right-most side, meaning a very efficient compressor, being represented by the smallest bubble, denoting absence of unfeasible camber angles; and blue, signifying a controlled diffusion.

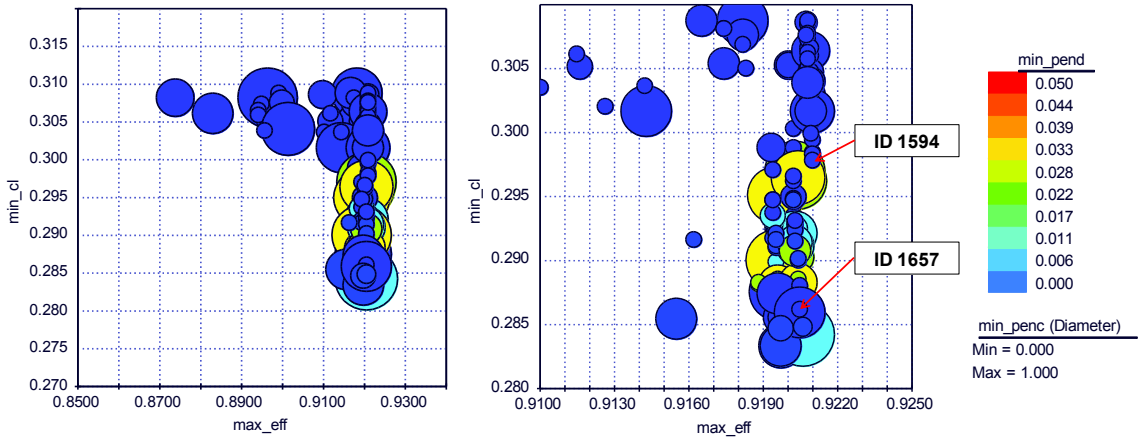

Figure 5. Bubble 4-D of some solutions, indicating ID 1594 and ID 1657.

The design 1594 gives a compressor with 92% efficiency and no penalty due to camber angle, nor diffusion factor. Nevertheless, the outlet gas angles are quite high, over 40°, requiring further investigation or the installation of an outlet guide vane (OGV) to reduce the undesirable high swirl velocity prior to the combustion chamber.

Similarly, the design 1657 gives a high-efficient compressor with 92.05% efficiency and no aforementioned penalties. Likewise, it does also have high gas outlet angles, what should require similar approaches as form ID 1594.

The comparison of the diffusion factor and camber angle from the initial design and the optimized ones are shown in Fig. 6.

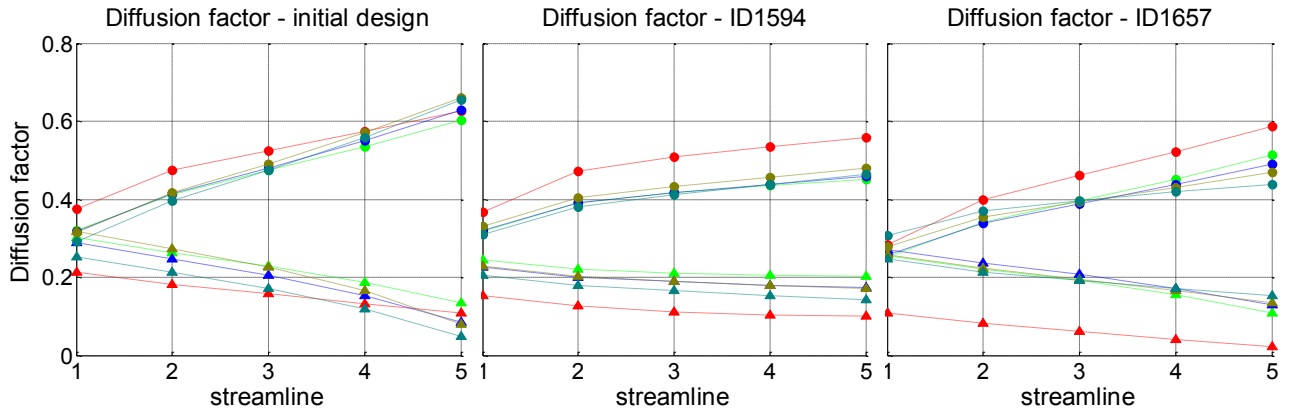

Figure 6. Difusion factor distribution from the initial non-optimized compressor, ID 1594 and ID 1697.

Noticeably, the diffusion factor distribution is significantly improved. In ID 1594 every node has diffusion factor below 0.6, as required. In a similar manner, the camber angle distribution has also benefited from the MOGA search, as the selected designs present angles all below the 40° limit – Fig. 7. However, the issue of high gas outlet angle is still present.

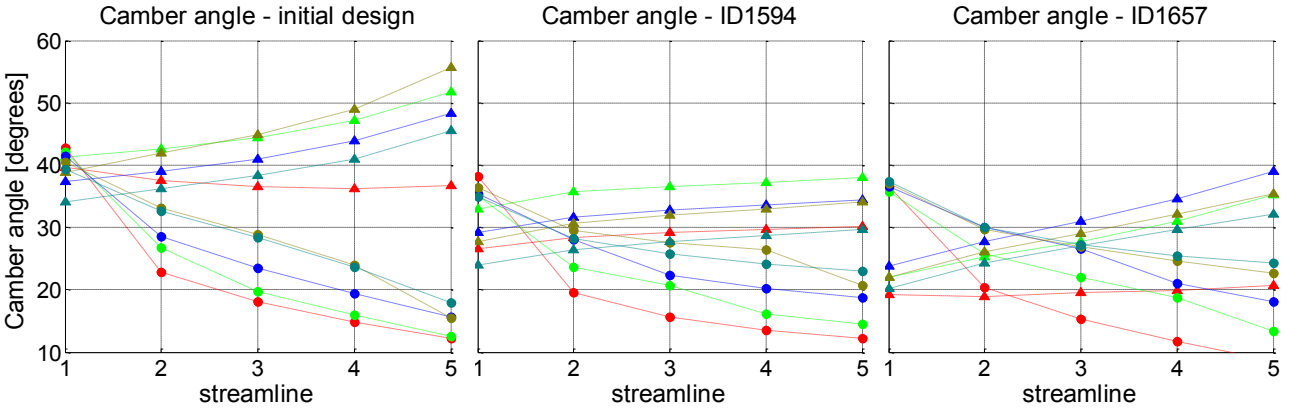

Figure 7. Camber angle distribution from the initial non-optimized compressor, ID 1594 and ID 1657.

Using 50 generations and 24 concurrent designs, totaling 1800 designs, it might be strange to focus in only two designs. Firstly, considering only the solutions that achieved a 'relaxed restriction' of allowing 1.0° of camber angle penalty and 0.05 of diffusion factor penalty, one gets 170 designs. From them, Tab. 6 indicates a high similarity among the 'relaxed solutions', where *eff_in* is the input isentropic efficiency, *htr* is the hub to tip ratio, *eff_calc* is the calculated efficiency, *penc* is the camber angle penalty and *pend* is the diffusion factor penalty.

Table 6. Similarity of the designs with 'relaxed restriction'.

	eff_in	$f_{imax,jmax}$	$f_{imax,jmin}$	$f_{imin,jmax}$	$f_{imin,jmin}$	htr	eff_calc	length	penc	pend
minimum	0.873	37.1	37.6	1.2	8.3	0.581	0.8736	0.2833	0.00	0.00
maximum	0.920	44.3	47.3	34.0	19.5	0.600	0.9210	0.3089	0.99	0.04
average	0.917	41.7	43.8	20.4	16.3	0.597	0.9175	0.2963	0.16	0.01
σ	0.008	1.4	2.1	8.9	3.2	0.003	0.0079	0.0077	0.27	0.01

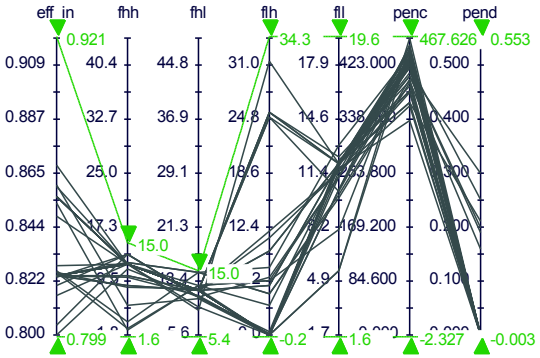

Figure 8. Parallel coordinates to filter designs with low values of gas outlet angle.

Considering the high gas outlet angles, another interesting search was for designs with lower aforementioned angles. This search lead to no design, which can be visually seen by the filter of Fig. 8, where *fhh* indicates the node at the tip of the last stage; *fhl*, the node at the hub of the last stage; *flh*, the node at the tip of the first stage and *fll* the node at the hub of the first stage. The filter is considering only the designs with *fhh*<15° and *fhl*<15°, but all those designs have undesirably high values of camber angle penalty, with values above 337° of penalty.

8. CONCLUSION

The study on the use of a Multi-Objective Genetic Algorithm in the design optimization of axial-flow compressors revealed positive. The design space could be widely explored in a much faster way and the use of a non-deterministic optimization approach lead to considerably more efficient designs. The automation obtained saves large amount of work hours and permits more sophisticated analysis and indicates useful tendencies. This study shows that the method is consistent and a deeper look at the design parameters should be conducted.

9. ACKNOWLEDGEMENTS

The authors would like to express their gratitude to Fundação de Amparo à Pesquisa do Estado de São Paulo – FAPESP – for the financial support to the project.

10. REFERENCES

Ando, V.F., 2010, “Project optimisation of high-performance axial flow compressor”, B.Sc. Thesis, Instituto Tecnológico de Aeronáutica, São José dos Campos.

Barbosa, J.R., 1987, “A Streamline Curvature Computational Programme for Axial Compressor Performance Prediction”, UK, Cranfield, Cranfield Institute of Technology.

Cohen, H.R., Rogers, G.F.C., Saravanamuttoo, H.I.H., 1996, “Gas Turbine Theory”, 4ª, Longmann, Essex.

Deb, K., 2002, “Multi-Objective Optimization using Evolutionary Algorithms”, John Wiley & Sons, Chichester.

Figueiredo, J.S., 2010, “Determination of Stall and Choke Limits of Transonic Axial Flow Compressor Using the Streamline Curvature Method”, M.Sc. Thesis, Instituto Tecnológico de Aeroáutica, São José dos Campos.

Griepentrog, H.R., 1970, “Secondary Flow losses in axial compressors”, AGARD LS 39.

Johnsen, I.A., Bullok, R.O., 1965, “Aerodynamic Design of Axial-Flow Compressors”, NASA SP-36, Washington, D.C.

Monsarrat, N.T., Keenan, M.J., Tramm, P.C. 1969, “Design Report – Single stage evaluation of highly loaded high Mach number compressor stages”, NASA CR-72562, Cleveland, Ohio.

Swan, W.C. 1961, “A practical method of prediction transonic compressor performance”, s.1, J. Eng. Power.

11. RESPONSIBILITY NOTICE

The authors are the only responsible for the printed material included in this paper.